Aalborg Universitet

AALBORG UNIVERSITY

A Unified Power Control Method for Standalone and Grid Connected DFIG-DC System

Wu, Chao; Cheng, Peng; Ye, Yuhua; Blaabjerg, Frede

A Unified Power Control Method for Standalone and Grid Connected DFIG-DC System

Chao Wu, *Member, IEEE*, Peng Cheng, Yuhua Ye, Frede Blaabjerg, *Fellow, IEEE*

Abstract—This letter proposes a unified power control method for DFIG-DC system, which can seamlessly transfer from grid connected mode to standalone mode without changing control strategy and vice versa. There is no need to detect the interconnection switch to identify whether it is grid connected or standalone. The dc voltage and stator active power are both positive correlations with the magnitude of rotor current vector, which indicates that these two objectives can be combined as the unified power to generate the rotor current reference. The stator frequency can be controlled by the rotating speed of rotor current vector without calculating stator frequency which can reduce the parameter dependency. Finally, the experiments based on a 1 kW DFIG-DC setup is carried out to verify the proposed unified power control method.

Index Terms— Doubly-fed induction generator (DFIG), grid connected mode, standalone mode, unified power control

I. INTRODUCTION

The rapid development of doubly-fed induction generator (DFIG) based wind farm and increasing adoption of dc transmission call for research in the topologies and control strategies of DFIG connected to dc grid [1]-[3]. Compared with other squirrel cage induction generators (SCIG) or permanent magnet synchronous generators (PMSG) based topology applied in dc system, the DFIG-DC topology, in which only one derated PWM converter is needed, has been widely studied due to its simple structure and reduced converter rating. There are mainly two operation modes of DFIG-DC system: grid connected mode and standalone mode.

Grid connected mode means the dc voltage is constant, where the main control objective is stator frequency and output power control. In [4]-[5], the stator frequency and torque are decoupling controlled based on calculating stator flux angle. In [6]-[7], a stator flux PLL is proposed for the decoupling control of stator frequency and torque which can avoid calculating stator frequency. However, this control method is dependent on the ratio of mutual inductance and stator inductance. Furthermore, all these control methods are based on constant dc

voltage without considering standalone mode.

In standalone mode, the dc voltage is not constant which needs to be controlled additionally [8]-[12]. In [8], the dc voltage is controlled through regulating the magnitude of stator flux and the stator flux orientation is attained by controlling *q*-axis stator flux to be zero. In [9]-[10], rotor active current is applied for regulating dc voltage without stator current sensors. In [11], a direct torque control scheme is proposed for dc voltage regulation based on hysteresis controller and optimal switching table. In [12], a mathematical model of DFIG-DC system considering harmonic currents in rotor flux reference frame is built for the better understanding of dc voltage control and torque ripple mitigation. However, the control accuracy of all these methods is highly dependent on machine parameters due to the stator or rotor flux orientation [8]-[12].

In conclusion, all the existing works are studying grid connected mode or standalone mode separately, and there is no work aimed to combine these two operation modes. In this letter, a unified power control method of DFIG-DC system for both standalone and grid connected operation is proposed without detecting the status of interconnection switch or changing control strategy. Furthermore, the unified power control is based on rotor current oriented control, which has no parameter dependency compared with other stator flux oriented methods. The rest of the letter is organized as follows.

First, the relationship between the stator power, dc voltage and the magnitude of rotor current vector is revealed in Section II through a mathematical model. In Section III, the unified power control method for both the power control in grid connected mode and dc voltage control in standalone mode is elaborated. The control performance analysis is presented in Section IV and the experimental results in Section V to validate the proposed strategy. In conclusion, a seamless transition between these two modes can be obtained without changing the control strategy.

II. SYSTEM LAYOUT AND MATHEMATICAL MODEL

The DFIG-DC system topology is illustrated in Fig. 1. The battery is used for the start up for standalone mode which has been analyzed in [10]. When the diode rectifier conducts, the steady state equivalent circuit of DFIG connected to diode bridge is shown in Fig. 2. The rotor side converter (RSC) and rotor side of DFIG can be equivalent as a current source which is expressed as I_r, I_s and I_m represent the stator and exciting current. U_s and E_m represent the stator voltage and air gap voltage, L_m and $L_{s\sigma}$ represent the mutual inductance and stator leakage inductance, R_s represents the stator resistance.

Fig. 1. DFIG connected to a DC link using a diode rectifier.

In this letter, only the average stator power is considered, the harmonics in voltages and currents are both ignored. When the diode bridge is working in continuous conduction mode, the magnitude of stator fundamental voltage can be expressed as,

$$\left|\boldsymbol{U}_s\right| = \frac{2}{\pi} V_{dc} \qquad (1)$$

Fig. 2. Steady-state equivalent circuit of the DFIG-DC system.

Since the stator resistance compared with stator leakage inductance is small, it can be ignored. Thus, the air gap voltage can be calculated as,

$$\boldsymbol{E}_m = j\omega_s L_m \boldsymbol{I}_m = \boldsymbol{U}_s + j\omega_s L_{s\sigma} \boldsymbol{I}_s \qquad (2)$$

where ω_s is the stator angular frequency, which is also the rotating speed of rotor current vector.

Since the stator current is the same phase with stator voltage, the stator power can be calculated as,

$$P_s = \mathrm{Re}\left(\boldsymbol{U}_s \boldsymbol{I}_s\right) = \frac{L_m}{L_s}\left|\boldsymbol{U}_s\right|\left|\boldsymbol{I}_r\right|\cos\delta \qquad (3)$$

where δ is the angle between rotor current and stator voltage. As can be seen from (3), the stator power is proportional correlation with the magnitude of rotor current.

According to (2), the magnitude of stator fundamental voltage can be approximately calculated as,

$$\left|\boldsymbol{U}_s\right| = \left|\omega_s L_m \boldsymbol{I}_m - \omega_s L_{s\sigma} \boldsymbol{I}_s\right| \approx \omega_s L_m \left|\boldsymbol{I}_m\right| = \omega_s L_m \left|\boldsymbol{I}_r\right|\sin\delta \qquad (4)$$

Based on (1) and (4), the dc voltage can be expressed by the rotor voltage as,

$$V_{dc} = \frac{\pi}{2}\left|\boldsymbol{U}_s\right| = \frac{\pi}{2}\omega_s L_m \left|\boldsymbol{I}_r\right|\sin\delta \qquad (5)$$

As can be seen from (5), the magnitude of rotor current is proportional correlation with dc voltage, which indicates that the magnitude of rotor current can also be used for regulating the dc voltage. (3) and (5) are the mathematical foundation for the unified power control presented in Section III.

III. UNIFIED POWER CONTROL STRATEGY

The RSC control scheme for the DFIG-DC system is shown in Fig. 3. The control scheme can be divided into three parts: stator frequency control, power and dc voltage control, and rotor current control. The stator frequency control is applied for generating the angle of synchronous d-q frame, the power and

dc voltage control loop is used for generating the magnitude of rotor current vector, the rotor current control is the conventional inner current control loop. Thus, the key novelty of the control scheme is the power and dc voltage control and stator frequency control, which will be elaborated in details.

A. Stator frequency control

In steady state, the stator frequency is equal to the rotating speed of rotor current vector in stationary frame. Thus, the stator frequency can be controlled through the rotor slip angle, which is used for reverse Park transform of rotor voltage. The rotor slip angle can be expressed as,

$$\theta_{slip} = \frac{1}{s}\omega_s^* - \theta_r \qquad (6)$$

where ω_s^* is the reference of stator angular frequency and θ_r is the rotor angle.

The q-axis rotor current is controlled to zero to maintain that magnitude of rotor current is equal to d-axis rotor current. Thus, the reference of q-axis rotor current is zero, which can be seen from Fig. 3.

Fig. 3. Unified power control method of RSC.

Fig. 4. The detailed block diagram of power and dc voltage control.

B. Power and dc voltage control

The detailed block diagram of power and dc voltage control is shown in Fig. 4. Since the q-axis rotor current is controlled to be zero, the d-axis rotor current is the magnitude of rotor current. As can be seen from (3) and (5), the stator power and dc voltage can both be controlled by the magnitude of rotor current. The dc voltage can also be controlled through the stator power, thus, a unified power reference can be generated by combing these two objectives with different coefficients under different working conditions.

When it is grid connected, the DFIG is working as power source. The unified power reference should be the same with power reference. When the dc grid is disconnected, the dc voltage will deviate from the rated value if it is still just the power reference due to the unknown dc load. The unified power P_{ssum} should be a combination of power reference and output of

dc voltage PI controller, which can be expressed as,

$$P_{ssum} = \alpha P_{dc} + P_s^* = \alpha \frac{k_{pv}s + k_{iv}}{s}\left(V_{dc}^* - V_{dc}\right) + P_s^* \quad (7)$$

where P_{dc} is the output of dc voltage controoler, k_{pv} and k_{iv} are the proportional and integral gain of dc voltage controller, α is a coefficient between 0 and 1.

The coefficient α is determined by the dc voltage error as,

$$\alpha = \frac{\left|V_{dc}^* - V_{dc}\right|}{V_{dc}^* \cdot e} \quad (8)$$

where e represents the steady state error of dc voltage, which is a flexible setting according to the practical requirement. In this letter, it is set as 2%, which means that the error of dc voltage in standalone mode is less than two percent of rated dc voltage. It should be noted that since the dc voltage error in standalone mode always exist, the output of dc voltage controller will be saturated. Since the output is power reference, which should be smaller than the rated power. Thus, the saturation value of the dc voltage controller is set as 1 pu.

When it is grid connected mode, the dc voltage is the same with the voltage reference, α is zero, thus the power reference can be accurately tracked. When it is standalone mode, the dc voltage is not the same with dc voltage reference, α is not zero and the dc voltage control loop will start to play a role and control the dc voltage to the given range. This means that the dc voltage PI controller only works when the dc voltage error exceed the setting error range. Furthermore, due to the stator side diode bridge, the dc voltage contains 6th order harmonic in the standalone mode. Thus, a 6th order harmonic notch filter should be added after the dc voltage error for the dc voltage control loop when the dc capacitor is small.

IV. CONTROL PERFORMANCE ANALYSIS

In this section, the control performance of the unified power control strategy in different operation mode are analyzed. It can be divided into grid connected mode and standalone mode.

When it is grid connected mode, namely the switch in Fig.1 is closed, the dc voltage is equal to the voltage reference. Thus, α is zero which means the dc voltage control loop is not working in this condition. The unified power is dependent on given power reference which can achieve the MPPT control of DFIG.

$$P_{ssum} = P_s^* \quad (9)$$

It should be noted that there are two PI controllers in this mode, the bandwidth of rotor current control loop is designed as 100 Hz and the bandwidth of power control loop is designed as 20 Hz. The detailed design procedure has been analyzed in [13], which is not repeated in this letter.

During the standalone mode, α is equal to 1 when the dc voltage error exceeds the setting range. As can be seen from Fig. 4, the power control loop is the inner loop of the voltage control loop. The bandwidth of the voltage control loop can be set smaller than the power control loop, thus the power control loop can be considered as unity gain to simplify the parameter design of the voltage control loop. In this way, the voltage control loop can be simplified as Fig. 5, where $slip$ represents the slip rate which is 0.1 in the experimental results, R_L is the dc load, i_{dc} is

the total dc current from DFIG to dc side, P_{base} and U_{base} are the base value of power and voltage respectively. The voltage controller is designed in per-unit control and the unit of dc voltage reference is also in per-unit.
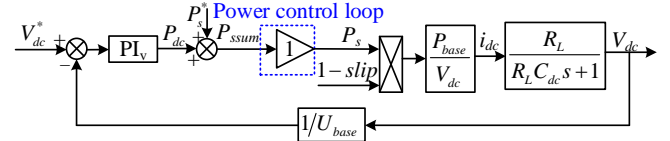

Fig. 5. Simplified dc voltage control diagram in standalone mode.

According to Fig. 5, the open loop transfer function of the dc voltage control loop can be deduced as,

$$G_o\left(s\right) = \frac{\left(1 - slip\right)P_{base}}{V_{dc} \cdot U_{base}} \frac{k_{pv}s + k_{iv}}{s} \frac{R_L}{R_L C_{dc} s + 1} \quad (10)$$

In order to ensure there is no voltage overshoot during the dynamic process. The voltage control loop is designed as a first-order block. Thus, the zero point of voltage PI controller should counteract the pole of the dc part. Since the dc load can change between 0 pu to 1 pu. The dc load equal to 0.5 pu was chosen for the controller design. Since the bandwidth of the power control loop is designed as 20 Hz, the voltage control bandwidth is designed as 5 Hz, which is 10π rad/s and expressed as ω_{bv}, R_L=40 Ω, C_{dc}=780 μF, P_{base}= 667 W, U_{base}=90 V, V_{dc}=140 V. Thus, the proportional and integral parameters can be obtained as,

$$k_{pv} = \frac{\omega_{bv}V_{dc}U_{base}C_{dc}}{\left(1 - slip\right)P_{base}} = 0.51, \, k_{iv} = \frac{\omega_{bv}V_{dc}U_{base}}{\left(1 - slip\right)P_{base}R_L} = 17 \quad (11)$$

In the steady state of standalone mode, α is less than 1. The unified power can be expressed as,

$$P_{ssum} = P_s^* + \alpha P_{dc} \quad (12)$$

Thus, the α can be expressed as,

$$\alpha = \frac{P_{ssum} - P_s^*}{P_{dc}} \quad (13)$$

Since the range of actual stator power P_{ssum} is between 0 pu to 1 pu, otherwise the stator current will exceed the rated value. The range of the stator power reference is also between 0 pu to 1 pu. In the steady state of standalone mode, the output of the dc voltage controller will be saturated to 1 pu due to the steady state error. Then, the relationship between α, the power reference and actual stator power can be plotted in Fig. 6.
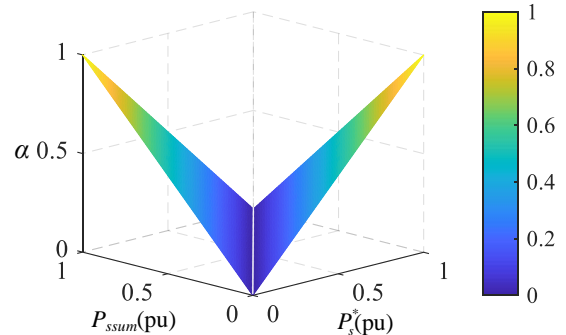

Fig. 6. The dc voltage error with various power reference and actual stator power in standalone mode.

As can be seen from Fig. 6, no matter what the power reference and actual stator power are, the dc voltage error in standalone mode is limited to the setting range, which is

determined by the error e in (8). Thus, the dc voltage can be controlled to the setting dc voltage range through the unified power control method.

V. EXPERIMENTAL RESULTS

In order to validate the unified power control method proposed in section III, a DFIG-based experimental system is developed shown as Fig. 7. The induction motor is worked as the prime motor of DFIG and is used to control the speed of DFIG. The control strategy of RSC is implemented on the TI TMS320F28335 DSP and the switching frequency is 10 kHz with a sampling frequency of 10 kHz. The parameters of the DFIG are shown in Table I. All the experimental waveforms are acquired by a YOKOGAWA DL750 scope.

TABLE I Parameters of the tested DFIG

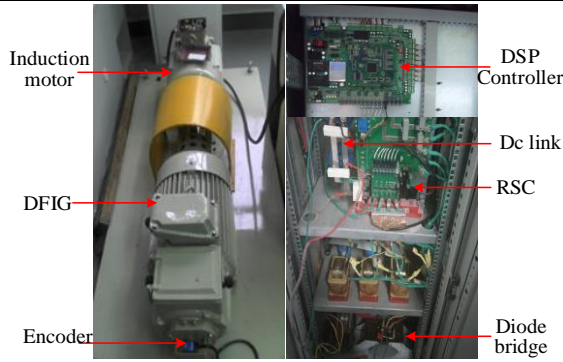| Parameters	Value	Parameters	Value
Rated power	1.0 kW	Rated voltage	110 V
Rated frequency	50 Hz	DC voltage	140 V
DC capacitance	780 μF	R_s	1.01 Ω
R_r	0.88 Ω	L_m	87.5 mH
$L_{\sigma s}$	5.6 mH	$L_{\sigma r}$	5.6 mH

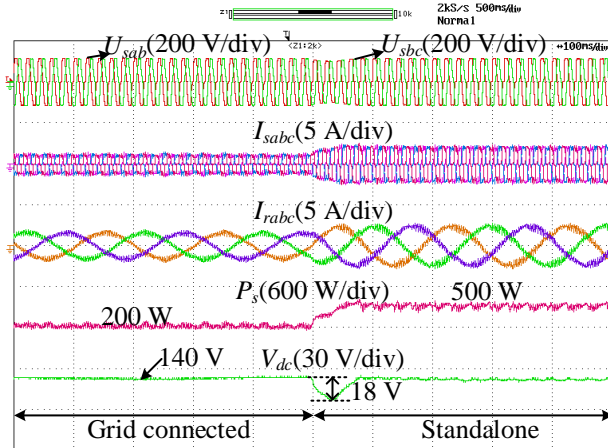Fig.7. Experimental set up of DFIG-DC system.

Fig. 8. Experimental results of DFIG from grid connected to standalone mode.

Fig. 8 shows the experimental results of DFIG from grid connected mode to standalone mode. At the beginning, the diode bridge is connected to dc grid and the dc voltage is a constant value at 140 V. The stator output power is set as 200 W and the stator frequency is set as 50 Hz. The rotor speed is 900 rpm. Suddenly, the dc grid is cut off and the DFIG automatically changes to the standalone mode, in which the

control objective is the dc voltage. Due to the load in standalone mode is larger than stator power reference , the dc link voltage will have a little fluctuation as 18 V drop but will come into steady state in 80 ms. The dc voltage error in the steady state is less than 1 V. According to Fig. 6, α is equal to 0.3, which means that the dc voltage error is 0.6%. This is consistent with experimental results, which validate the effectiveness of dc voltage control in standalone mode.

Fig. 9 shows the experimental results of DFIG changing from standalone to grid connected mode. The dc load is 500 W which should be entirely supplied by the DFIG when it is standalone mode. When the dc grid is connected, the dc voltage becomes 140 V as a constant value and the DFIG is working as a power source, thus the stator output power changes to 200 W in the grid connected mode. As can be seen from Fig. 8 and Fig. 9, the DFIG-DC system can work in both standalone and grid connected mode with the unified power control strategy.
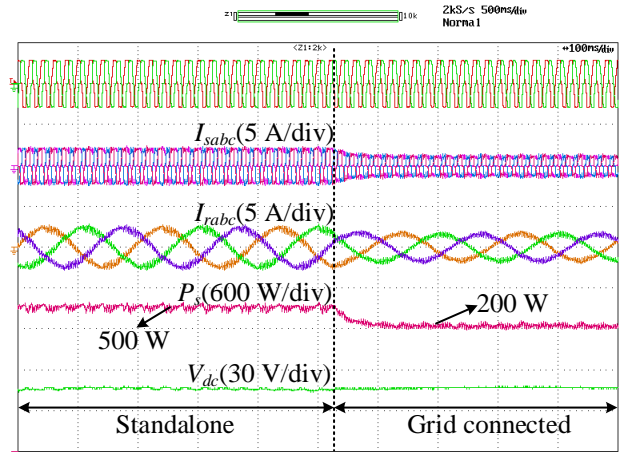

Fig. 9. Experimental results of DFIG from standalone to grid connected mode.

VI. CONCLUSION

A unified power control method for both grid connected and standalone DFIG-DC system is proposed in this letter. A unified power reference is built based on a combination of given power reference and dc voltage reference. This unified power control method is adaptive in both standalone and grid connected mode without changing the control strategy. Furthermore, the power control / dc voltage control and stator frequency control has no parameter dependency. In conclusion, this unified control method is a highly robust method for the DFIG-DC system in both stand alone and grid connected mode.

REFERENCES

[1] N. Yu, H. Nian, and Y. Quan, "A novel DC grid connected DFIG system with active filter based on predictive current control," in *Proc. Int. Conf. Elect. Mach. Syst.*, Aug. 22–23, 2011, pp. 4525–4537.

[2] H. Nian and X. Yi, "Coordinated control strategy for doubly-fed induction generator with dc connection topology," *IET Renew. Power Gener.*, vol. 9, no. 7, pp. 747–756, Aug. 2015.

[3] G. D. Marques and M. F. Iacchetti, "DFIG Topologies for DC Networks: A Review on Control and Design Features," *IEEE Trans. Power Electron.*, vol. 34, no. 2, pp. 1299-1316, Feb. 2019.

[4] M. F. Iacchetti, G. D. Marques, and R. Perini, "Torque ripple reduction in a DFIG-DC system by resonant current controllers," *IEEE Trans. Power Electron.*, vol. 30, no. 8, pp. 4244–4254, Aug. 2015.

[5] H. Nian, C. Wu, and P. Cheng, "Direct resonant control strategy for torque ripple mitigation of DFIG connected to DC link through diode rectifier on

This article has been accepted for publication in a future issue of this journal, but has not been fully edited. Content may change prior to final publication. Citation information: DOI 10.1109/TPEL.2020.2996267, IEEE Transactions on Power Electronics

5

stator," *IEEE Trans. Power Electron.*, vol. 32, no. 9, pp. 6936–6945, Sep. 2017.

[6] C. Wu and H. Nian, "Sinusoidal current operation of DFIG-DC System without stator voltage sensors," *IEEE Trans. Ind. Electron.*, vol. 65, no. 8, pp. 6250–6258, Aug. 2018

[7] C. Wu, H. Nian, "An Improved Repetitive Control of DFIG-DC System for Torque Ripple Suppression," *IEEE Trans. on Power Electron.*, vol. 33, no.9, pp. 7634-7644, Sep. 2018.

[8] H. Misra, A. Gundavarapu, and A. K. Jain, "Control scheme for DC voltage regulation of stand-alone DFIG-DC system," *IEEE Trans. Ind. Electron.*, vol. 64, no. 4, pp. 2700–2708, Apr. 2017.

[9] G. D. Marques and M. F. Iacchetti, "Sensorless frequency and voltage control in stand-alone DFIG-DC system," *IEEE Trans. Ind. Electron.*, vol. 64, no. 3, pp. 1949–1957, Mar. 2017.

[10] H. Misra and A. K. Jain, "Analysis of stand alone DFIG-DC system and DC voltage regulation with reduced sensors," *IEEE Trans Ind. Electron.*, vol. 64, no. 6, pp. 4402–4412, Jun. 2017.

[11] A. Gundavarapu, H. Misra, and A. K. Jain, "Direct torque control scheme for DC voltage regulation of the standalone DFIG-DC system," *IEEE Trans. Ind. Electron.*, vol. 64, no. 5, pp. 3502–3512, Apr. 2017.

[12] H. Misra and A. K. Jain, "Mathematical modeling and control of standalone DFIG-DC system in rotor flux reference frame," *IEEE Trans. Ind. Electron.*, vol. 65, no. 5, pp. 3708-3719, May 2018.

[13] C. Wu, Y. Jiao, H. Nian and F. Blaabjerg, "A Simplified Stator Frequency and Power Control Method of DFIG-DC System Without Stator Voltage and Current Sensors," *IEEE Trans. on Power Electron.*, vol. 35, no. 6, pp. 5562-5566, Jun. 2020.